

## Impact of Electric Fields on the Nanoscale Behavior of Lipid Monolayers at the Surface of Graphite in Solution

Hongmei Bi, Xuejing Wang, Xiaojun Han, and Kison Voitchovsky

*Langmuir*, **Just Accepted Manuscript** • DOI: 10.1021/acs.langmuir.8b01631 • Publication Date (Web): 20 Jul 2018

Downloaded from <http://pubs.acs.org> on July 23, 2018

### Just Accepted

"Just Accepted" manuscripts have been peer-reviewed and accepted for publication. They are posted online prior to technical editing, formatting for publication and author proofing. The American Chemical Society provides "Just Accepted" as a service to the research community to expedite the dissemination of scientific material as soon as possible after acceptance. "Just Accepted" manuscripts appear in full in PDF format accompanied by an HTML abstract. "Just Accepted" manuscripts have been fully peer reviewed, but should not be considered the official version of record. They are citable by the Digital Object Identifier (DOI®). "Just Accepted" is an optional service offered to authors. Therefore, the "Just Accepted" Web site may not include all articles that will be published in the journal. After a manuscript is technically edited and formatted, it will be removed from the "Just Accepted" Web site and published as an ASAP article. Note that technical editing may introduce minor changes to the manuscript text and/or graphics which could affect content, and all legal disclaimers and ethical guidelines that apply to the journal pertain. ACS cannot be held responsible for errors or consequences arising from the use of information contained in these "Just Accepted" manuscripts.



# Impact of Electric Fields on the Nanoscale Behavior of Lipid Monolayers at the Surface of Graphite in Solution

*Hongmei Bi<sup>a</sup>, Xuejing Wang<sup>b</sup>, Xiaojun Han<sup>\*b</sup> and Kislun Voïtchovsky<sup>†c</sup>*

<sup>a</sup>College of Science, Heilongjiang Bayi Agricultural University, Daqing 163319, China

<sup>b</sup> State Key Laboratory of Urban Water Resource and Environment, School of Chemistry and Chemical Engineering, Harbin Institute of Technology, Harbin 150001, China.

<sup>c</sup> Department of Physics, Durham University, Durham DH1 3LE, UK.

**ABSTRACT:** The nanoscale organization and dynamics of lipid molecules in self-assembled membranes is central to the biological function of cells and in for the technological development synthetic lipid structures as well as in devices such as biosensors. Here we explore the nanoscale molecular arrangement and dynamics of lipids assembled in monolayers at the surface of highly ordered pyrolytic graphite (HOPG), in different ionic solutions and under electrical potentials. Using a combination of atomic force microscopy and fluorescence recovery after photobleaching, we show that HOPG is able to support fully formed and fluid lipid membranes, but mesoscale order and corrugations can be observed depending on the type of lipid considered (DOPC, DOPS, DOTAP) and the ion present ( $\text{Na}^+$ ,  $\text{Ca}^{2+}$ ,  $\text{Cl}^-$ ). Interfacial solvation forces and ion-specific effects dominate over the electrostatic changes induced by moderate electric fields ( $\pm 1.0$  V versus Ag/AgCl reference electrode) with particularly marked effects in the presence of calcium, and for DOPS. Our results provide insights into the interplay between molecular, ionic and electrostatic interactions and the formation of dynamical ordered structures in fluid lipid membranes.

**KEYWORDS:** Lipid membrane, HOPG, Electrochemistry, Metal ions, Water, Atomic force microscopy

**Introduction**

Biological membranes (biomembranes) are primarily composed of lipids and membranes proteins self-assembled into a complex two-dimensional structure that can evolve in response to external stimuli and actively support the cell function.<sup>1</sup> By efficiently separating the inside of the cell from the surrounding environment, biomembranes are able to actively sustain a significant trans-membrane electrical potential; the primary source of energy for the cell. This trans-membrane potential also plays an important role in protein function<sup>2,3</sup> as well as the activation of many biological processes.<sup>4</sup> Additionally, since many membrane components are electrically charged, external electric fields can provide a driving force for the motion of components based on electrophoresis, electroosmosis and hydrodynamic flow.<sup>5-9</sup> The central role of biological membranes in cell function is underlined by the fact that they constitute a primary drug target<sup>10</sup> and countless studies have investigated functional aspects of the nanoscale organization of different proteins and lipids.<sup>11, 12</sup> However, the complexity and delicate nature of most native membranes renders *in-situ* nanoscale studies challenging, especially when considering phenomena related to ionic effects<sup>13-15</sup> and to the trans-membrane potential. To date, few studies have been able to explore molecular-level details of membranes under an electrical potential, and investigations are typically conducted on membrane fragments or synthetic model membranes supported on a flat solid.<sup>16, 17</sup> Changes in the membrane molecular assembly and the structure of its components in response electric fields can provide important clues about the how trans-membrane potentials impact the behavior and function of living cells. The use of supported membranes is particularly helpful for high-resolution studies because it limits the spatial fluctuations natural to cell membranes, and the support can be directly used as an electrode for imposing a controlled trans-membrane potential.<sup>18, 19</sup> Supported membranes are routinely used as

1  
2  
3 model systems for nanoscale investigations with techniques such as fluorescence and super-  
4 resolution microscopies<sup>20</sup> and atomic force microscopy (AFM).<sup>21,22</sup> AFM can simultaneously offer  
5 molecular-level topographical and mechanical information about the membrane,<sup>23-25</sup> it can be  
6 combined with most optical microscopies and is fully compatible with electrochemical  
7 measurements on membranes.<sup>26-29</sup>

14 Details of the electrochemical behavior of model membranes and lipid bilayers assembled on  
15 gold substrates have already been reported,<sup>30-35</sup> also using AFM.<sup>14-16, 33-38</sup> Results have shown a  
16 potential-induced slow structural transformation of the membrane until a characteristic corrugated  
17 phase appears.<sup>36</sup> The overall stability of the membrane depends on the magnitude of the applied  
18 electrical potential; studies with model DMPC-Cholesterol (1,2-dimyristoyl-*sn*-glycero-3-  
19 phosphocholine-Cholesterol) bilayers<sup>21</sup> demonstrated a stability limit of -0.3 V, with membrane  
20 swelling observed beyond -1.0 V. Results are however dependent on the membrane composition  
21 and AFM spectroscopy on lipid bilayers with increasing ganglioside content<sup>37</sup> showed a transition  
22 from a corrugated to a homogeneous phase, with an associated increase in the bilayer thickness  
23 (from ~5.3 to 7.3 nm). The use of gold electrodes can be problematic in the context of  
24 biomembranes, first because biomolecules tend to adhere non-specifically to gold, often resulting  
25 in the deformation or denaturation of the molecules.<sup>38-40</sup> Additionally, the fabrication of gold  
26 electrodes makes it often difficult to achieved large area that is atomically flat. The surface of the  
27 electrode is typically composed of multiple small crystals exposing the Au (111) facet and able to  
28 reconstruct rapidly in ambient conditions.<sup>21, 33, 37, 41, 42</sup> There are examples of measurement with  
29 polycrystalline gold electrodes exhibiting large surfaces of Au(111) and good bilayer stability,<sup>43</sup>  
30 but these are not the norm. These issues can be overcome with liquid metal mercury electrodes.  
31 This strategy has been successfully used for developing fundamental theories about phase behavior  
32  
33  
34  
35  
36  
37  
38  
39  
40  
41  
42  
43  
44  
45  
46  
47  
48  
49  
50  
51  
52  
53  
54  
55  
56  
57  
58  
59  
60

of lipids under electric fields<sup>44-46</sup> and investigating channel transport of ions.<sup>47-54</sup> Various experimental strategies have been reported such as the use of wafer-based mercury film electrodes,<sup>55, 56</sup> the tracking of phase transition at different potentials using an silver/silver chloride (Ag/AgCl) reference<sup>57</sup> or recent direct measurement of the structural changes of lipid layers at electrified Hg surfaces using AFM spectroscopy.<sup>58</sup> Despite these successes, working with mercury electrodes remains highly challenging; the electrodes are inherently fragile and their long-term stability is uncertain. This renders the characterization of membranes' electrochemical behavior with microscopic techniques particularly difficult.<sup>51, 59</sup> Graphite offers a practical and cost-effective alternative to noble metal electrodes. Highly oriented pyrolytic graphite (HOPG) can be easily cleaved immediately before an experiment, revealing an atomically flat, highly conducting, inert and clean surface spanning hundreds of micrometers. This makes HOPG is an excellent substrate for electrochemical AFM measurement, with examples spanning from the self-assembly of peptides<sup>60-62</sup> to single atom or ion investigations.<sup>63-67</sup> Yet, to the best of our knowledge, HOPG has never been used for the AFM investigations of lipid membranes under electric potentials. This may be down to the fact that HOPG is hydrophobic, hence allowing only the formation of a single lipid monolayers on its surface. However this can be seen as an advantage for investigation of nanoscale interfacial effects between the surface of bilayers and the surrounding solution because it ensures optimal stability of the supported layer.

In this work, we characterize the nanoscale structural changes of model lipid membranes supported on HOPG's basal plane under electrical potential using AFM, and explore the effect of the field in controlling the resulting lipid assembly. We conduct high-resolution imaging and force spectroscopy measurements on pure phospholipid monolayers with zwitterionic (phosphocholine), negatively charged (phosphoserine) and positively charged (trimethylammonium-propane)

headgroups. The AFM results are complemented by fluorescence recovery after photobleaching (FRAP) measurements quantifying the lipids mobility in the absence of electric field in order to confirm that the HOPG support does not significantly affect the properties of the lipids at rest.

## Experimental Section

### Materials

Neutral lipids (1,2-Dioleoyl-*sn*-glycero-3-phosphocholine, DOPC), negatively charged lipids (1,2-dioleoyl-*sn*-glycero-3-phospho-L-serine, DOPS), and positively charged lipids (1,2-dioleoyl-3-trimethylammoniumpropane, DOTAP) were purchased from Avanti Polar Lipids (Alabaster, USA) with purity >99%. All other reagents were of analytical grade and purchased from Sigma Aldrich (Gillingham, UK). The imaging solutions (150 mM NaCl, 150 mM CaCl<sub>2</sub>) were prepared with ultrapure water (Milli-Q, 18.2 OM, <5 ppm organics, Merck-Millipore, Billerica, MA, USA).

### Electrochemical System Setup

A bespoke electrochemical setup comprising three electrodes was developed for the experiments (Fig. 1). The working electrode is made of HOPG (SPI supplies, West Chester, PA) and act as support for lipid monolayer. The HOPG was glued with epoxy resin (Araldite, RS components, UK) onto a stainless steel disc (SPI supplies) for magnetic fixation to the AFM scanner, and electrical contact was made directly to the HOPG with a copper wire. The counter electrode was made of a thin platinum sheet (<1 µm thick, Gold Leaf Supplies, Bridgend, UK) uniformly

covering the back for the AFM cantilever holder except for a hole directly above the cantilever (Fig. 1).

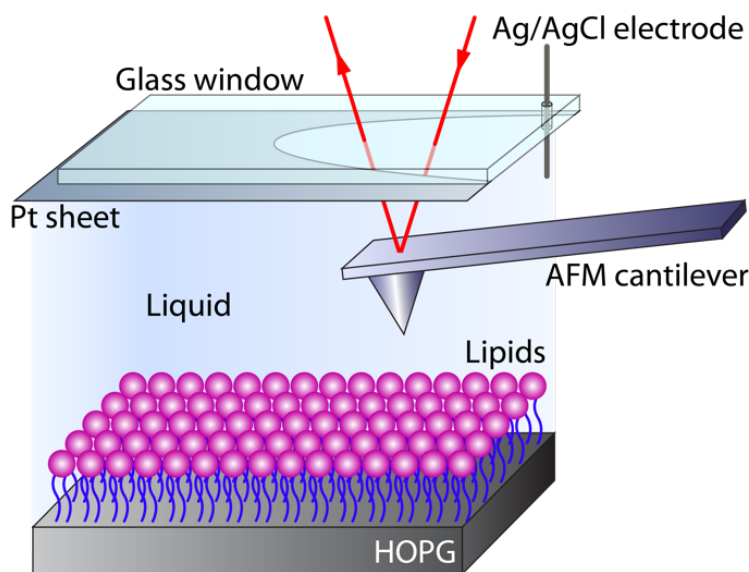


**Figure 1.** Schematic representation of the electrochemical AFM setup (not to scale). The HOPG substrate act as the working electrode, the platinum sheet lining the glass window of the cantilever holder is the counter electrode and the thin Ag/AgCl reference electrode is inserted through a hole located near the cantilever. The electric potential is applied by an Autolab electrochemical workstation.

This strategy ensured a uniform electric field while preventing any physical hindrance to the scanning tip and risk of short circuit. Additionally, the low cost of platinum sheets (typically < £0.1/cm<sup>2</sup> for high purity Pt) allows for routine replacement of the electrode if/when damaged. We used an Ag/AgCl reference electrode, prepared by electroplating fresh Ag wire (75 µm diameter, Sigma Aldrich, China) in 1.0 M KCl before every measurement. The current vs time curve of the Ag/AgCl reference electrode during this preparation (2 V applied potential) is shown in Fig. S1. All potentials in this paper are quoted versus the potential of this reference electrode (0.235V with respect to NHE) unless otherwise stated. The electrochemical measurements were conducted with and Autolab electrochemical workstation (PGSTAT204, Switzerland).



## Sample preparation

Supported lipid monolayers were formed via the vesicle fusion method.<sup>67-70</sup> In short, 2 mg of the desired lipids were dried overnight under vacuum in a glass vial and subsequently re-hydrated in 1 mL distilled water under ultrasound. Extrusion was conducted with a 100 nm filter (Whatman, GE Healthcare Life Sciences, Buckinghamshire, UK) using a mini-extruder kit (Avanti Polar Lipids). A mixture comprising 20  $\mu$ L of the extruded solution and 100  $\mu$ L of 150 mM NaCl solution was deposited onto a freshly cleaved HOPG and allowed to incubate at room temperature for 40 min. The exposed surface of HOPG is overwhelmingly composed of its basal plane apart from occasional step edges. The sample was then gently rinsed with 2 mL of the desired solution (ultrapure water, 150 mM NaCl, or 150 mM  $\text{CaCl}_2$ ). If necessary, more imaging solution was added before the experiment. The sample was then placed into the AFM's imaging cell for a 20 minutes thermal equilibration period at  $25.0 \pm 0.1$  °C, immediately followed by the experiment. Given the temperature of the experiments, all lipid membranes are expected to be in fluid phase when at rest. Generally, the membranes appear fully stable on the HOPG substrate, with no noticeable changes over the duration of the experiments and after storage for up to 6 hours.

## AFM experiments

All AFM data were acquired on a Cypher ES system (Asylum Research, Santa Barbara, CA, USA) with the sample and the cantilever/tip fully immersed in the imaging solution.<sup>71, 72</sup> The cantilevers used for the experiments (RC800 PSA, Olympus, Tokyo, Japan) have a nominal spring constant of 0.1 N/m. They were further calibrated using their thermal spectrum to ensure comparability of the force measurements. During imaging, the cantilever was oscillated using photothermal excitation (blue drive) for more accuracy and stability. The relatively low resonance

frequency of the first eigenmode in solution ( $\sim 4$  kHz) renders low noise imaging difficult. The cantilever was hence generally driven at its second vibration eigenmode ( $\sim 35$  kHz in solution). All images were taken at a constant scan rate (lines-per-second) of 2.44 Hz. Force spectroscopy measurements were conducted with a tip approach velocity of 200 nm/s and the maximum applied force was controlled with a trigger. The samples were kept at  $25.0 \pm 0.1$  °C using an in-built temperature control system. Analysis of the AFM results was conducted in Igor Pro (Wavemetric, Lake Oswego, USA) using home-programmed routines. The membrane rupture force, derived from force-distance spectroscopy measurements, was directly calculated using a semi-automated procedure able to identify steps and combine the results from multiple curves into suitable histograms (see Supplementary Fig. S2 for a detailed example).

### Fluorescence recovery after photobleaching (FRAP) experiments

The FRAP measurements were conducted on HOPG-supported lipid monolayers to quantify the lipid mobility in each experimental condition. The monolayers are expected to be in fluid state. A fluorescently labelled lipid (DPPE-Rhod, Avanti Lipids) was added to the lipid monolayer (0.04%, molar ratio) during the vesicles formation. Its low concentration does not affect the overall lipid fluidity but the Rhodamine tag provides the fluorescence needed<sup>63</sup> for the mobility measurement. A confocal fluorescence microscope (Nikon UK, Kingston, UK) was used to image the monolayer in reflection mode and carry out FRAP measurements, including after rinsing with different solution. The fluorescence recovery was analyzed over a  $20 \times 20 \mu\text{m}^2$  bleaching spot. At least three separate measurements were carried out for each sample and subsequently averaged so as to derive reliable and statistically meaningful results. The data analysis was conducted in ImageJ (version 1.44p).<sup>73</sup> The lateral diffusion coefficient  $D$  was calculated using the following equation:<sup>70, 74, 75</sup>

$$D = 0.224 R^2/t_{1/2} \quad (1)$$

Where  $D$  is in  $\mu\text{m}^2/\text{s}$ ,  $R$  is the radius of the bleached spot in  $\mu\text{m}$  and  $t_{1/2}$  (s) is the half-life of fluorescence recovery. This formula takes into account a correction and fitting due to the geometry of the bleaching.<sup>63, 76, 77</sup>

## Results and Discussion

### 1. AFM measurements

Hereafter the three different lipids (DOPC, DOPS, DOTAP) are investigated sequentially, each in different solutions and for applied potentials of 0 V and  $\pm 1.0$  V to the HOPG working electrode. The electrochemical stability of the HOPG surface itself was first tested over the same potentials in 150 mMNaCl(Fig. S3) confirming no degradation or noticeable changes in its atomic features.

**Electrically neutral monolayers** were prepared with zwitterionic DOPC lipids (see experimental section). Representative AFM micrographs of the monolayers obtained with applied potentials of 0.0 V, -1.0 V and +1.0 V are shown in Figure 2. In all cases, a topographic image of the membrane is presented, together with a typical example of a force-distance curve where the AFM tip is able to rupture the monolayer by pressing perpendicularly to its surface. A statistical analysis of the rupture forces derived from >10 curves (typically 30) is also shown with histogram of the resulting average value and its spread. No obvious features such as domain or corrugation are visible in topography, except for the occasional horizontal scanning streak characteristic of AFM over fluid membranes. No obvious structural transformation of the membrane could be observed under electric fields and the DOPC membrane remained fully fluid over all our experimental condition (25 °C). This contrasts with previous reports of significant structural transformations for phosphocholine-based bilayers on electrified gold electrodes.<sup>21, 78</sup> While the

lipids used in present system are expected to be more fluid, some structural rearrangements in the membrane are still present. The zwitterionic nature of the phosphocholine headgroup makes it polar and its orientation is sensitive to the electrostatic environment. This results in local electric field being able to shift the average molecular arrangement in the membrane and the transition temperature of phosphocholine bilayers.<sup>79</sup> Here, this translates into significant differences in the observed rupture force, depending on both the ionic environment and the applied electric field.

In NaCl, the impact of the applied potential is minimal with a slight increase (~15%) of the rupture force at  $\pm 1.0$  V. This changes dramatically in pure water due to the lack of electrostatic screening. In the absence of an applied potential, the rupture force increases by a factor  $\sim 2$ , presumably due to the surface potential of the immersed tip (typically -60 mV).<sup>80-83</sup> We note that given the different experimental conditions and tip compared to NaCl, an absolute comparison of the rupture force values should be done with caution. Nonetheless, the impact of the applied potential (directly comparable) is significant, inducing an increase  $> 250\%$  of the rupture force for both  $\pm 1.0$  V. Additionally, the membrane rupture process exhibit some sub-steps less than a nanometer wide (blue and red arrows), suggesting some structural rearrangement of the phosphocholine headgroup under the tip pressure. These results are consistent with the idea of electrically induced re-arrangement of the lipid packing.<sup>79</sup> Results in  $\text{CaCl}_2$  exhibit a behavior closer to that of NaCl, but with lower rupture forces under applied electric fields and an asymmetrical behavior at positive and negative bias, presumably reflecting the difference in valency between the  $\text{Ca}^{2+}$  cation and the  $\text{Cl}^-$  anion. A high rupture force variability was observed in the absence of applied fields with the most common value (histogram maximum) exhibiting a larger rupture force than at  $\pm 1.0$  V. This high variability may be due to localized ionic effects

inducing mesoscale order in the membrane,<sup>63</sup> but the present results do not allow for a clear conclusion.

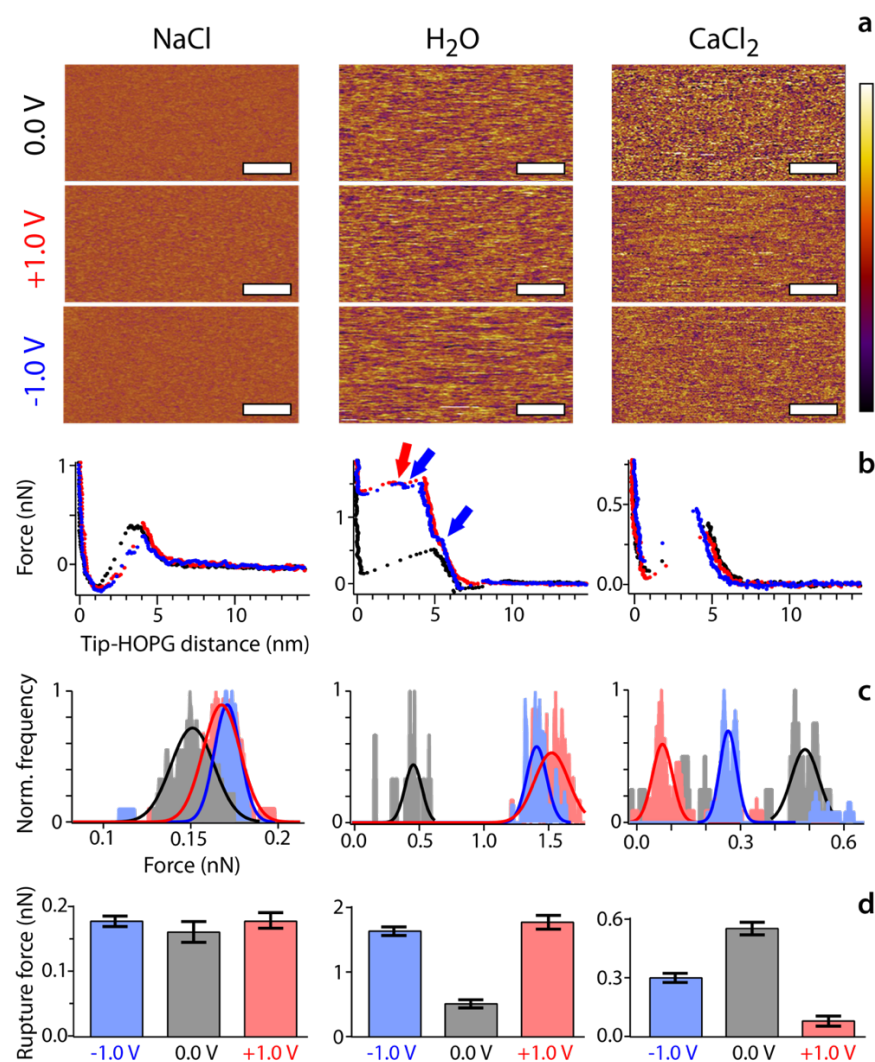


**Figure 2.** Impact of electric potentials on DOPC monolayers in different ionic solutions. In each solution, a representative topographic image is shown (a) and force distance curve exhibiting membrane rupture (b) is shown for applied potentials of 0 V (black), -1.0 V (blue) and +1.0 V (red). Arrows in (b) indicate sub-steps in the monolayer rupture process. Statistical analysis of >10 force-distance curves (c) reveals the most probable rupture force and its variability in each case (see Supplementary Fig. S2 for a detailed description of the statistical analysis). A Gaussian fit of the main peak is also shown. The value of the average rupture force derived from the fit is shown in (d). The displayed error is the derived width of the Gaussian from the fit. The scale bar is 20 nm in (a) and the color bar represents a height variation of 1.8 nm.

A quick look at Fig. 2b provides an idea of the DOPC membrane's apparent thickness in each condition, ranging from  $\sim 3$  nm at 0 V to 4-5 nm under a potential (from top to bottom of the step). This thickness is larger than expected for a DOPC monolayer, and a naive interpretation would rather suggest a bilayer. However, the presence of a bilayer on HOPG is highly unlikely in solution because the associated free energy would be considerably higher than for the lipids exposing their hydrophobic tail to the HOPG surface. Phospholipid bilayers typically rearrange into monolayers when in contact with a hydrophobic surface.<sup>84</sup> Alternatively, our results could indicate a triple lipid layer, with a bilayer directly on top of a monolayer at the interface with HOPG, but the  $\sim 3$  nm thickness observed in NaCl does not support this interpretation. Additionally, the intermediate steps visible in pure water when under electrical potential are significantly smaller than the thickness of a monolayer, supporting rather some structural rearrangement of the lipid headgroups and the associated hydration landscape probed by the tip. In light of these observations, we believe that our results are best explained by the presence of a lipid monolayer, potentially appearing larger due to its hydration layers and ionic effects are at play, especially when under an electrical potential. Hydrated ions are likely to influence the apparent membrane thickness and affect its hydration landscape, as illustrated by the  $\sim 2$  nm change in apparent membrane thickness between NaCl solution and pure water. Additionally, the fact that the substrate is hydrophobic makes absolute thickness measurements difficult because the tip progressively loses its hydration shell while pressing against the HOPG after having punctured the membrane. Results obtained at 0 V suggest a hydration thickness of  $\sim 1$  nm (distance between zero and step minimum). In principle statistical analysis of the apparent thickness at the rupture point is possible, but an approach similar to that used for extracting the rupture forces (Fig. 2c) provided unreasonable results for the reasons described above (not shown).

Generally, while our results are best interpreted by having a single DOPC monolayer on the HOPG surface together with significant hydration/ionic effects, we cannot exclude other interpretations and AFM-independent control experiments are needed to reach a definitive conclusion. We therefore conducted time-dependent electrical measurements (electrochemical impedance spectroscopy) on the system to quantify its capacitance (see supplementary Fig. S4 for details). We investigated each of the three types of lipid membranes as well as HOPG for reference, always in a 150 mM NaCl solution. The results indicate resistance values of 172 k $\Omega$  for bare HOPG, 306 k $\Omega$  for DOPC, 316 k $\Omega$  for DOPS, and 477 k $\Omega$  for DOTAP, confirming the formation of lipid membranes on the HOPG substrate. However, the corresponding membrane capacitances were found to be 8.15  $\mu\text{F}/\text{cm}^2$  (DOPC), 8.46  $\mu\text{F}/\text{cm}^2$  (DOPS) and 9.48  $\mu\text{F}/\text{cm}^2$  (DOTAP), more than four times larger than the expected for a perfect monolayer. Indeed, the characteristic capacitance of lipid bilayers ranges from 0.4 to 1  $\mu\text{F}/\text{cm}^2$ ,<sup>85, 86</sup> indicating that a monolayer capacitance should hence be typically ranging between 0.8 and 2  $\mu\text{F}/\text{cm}^2$ . This high apparent capacitance can be explained by defects in the monolayers, for example at step-edges of the HOPG due to its large surface area. The current leakage at these defects would artificially raise the observed capacitance values during the electrochemical impedance spectroscopy measurement, as observed here. In summary, while the impedance data tends to support the presence of a monolayer, it is also not fully conclusive.

**Negatively charged lipid monolayers** were created from DOPS using the same protocol as for DOPC. Figure 3 shows the effect of the different saline solution and electric field on the membrane topography. Unlike DOPC, the phosphoserine headgroups of DOPS appear to influence dramatically the molecular organization of the lipids in the membrane, depending on the local electrostatic environment. The AFM micrographs reveal clear structural changes such as periodic

corrugations in the form of parallel row-like features that could be observed in different experimental condition (Fig. 3a). These features are reminiscent of the hemi-micellar lipid structures reported in previous report.<sup>87-90</sup>

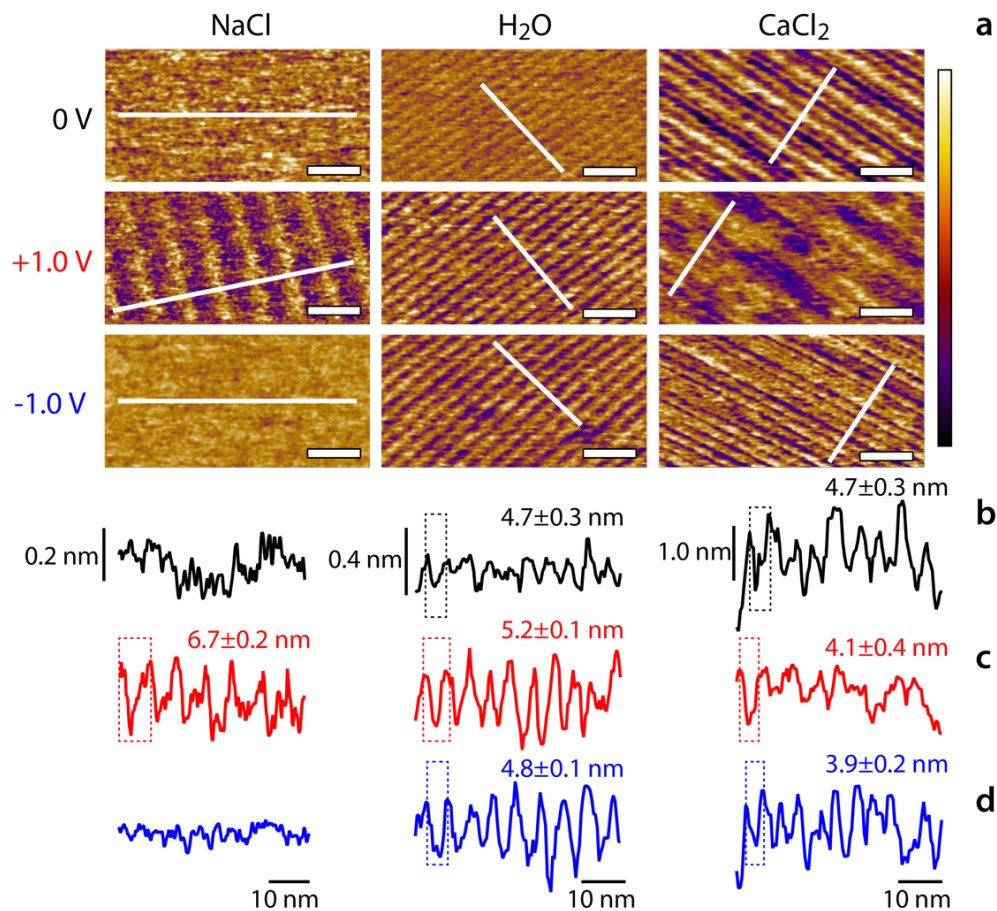


**Figure 3.** Impact of electric potentials on DOPS monolayers in different ionic solutions. In each solution, a representative topographic image is shown (a) together with a profile taken at 0 V (b), +1.0 V (c) and -1.0 V (d). For each profile exhibiting periodic corrugations a single corrugation is highlighted (dashed box) and the average periodicity length is given in inset. The scale bar is 20 nm in (a) and the color bar represents a height variation of 0.5 nm in NaCl, 1 nm in pure water and 2.5 nm in CaCl<sub>2</sub>.



1  
2  
3 In NaCl, the membrane appears completely homogenous in at 0 V and -1.0 V. When +1.0 V is  
4 applied to the HOPG electrode for about 15 min, faint corrugations with a periodicity of  $6.7 \pm 0.2$   
5 nm and a depth of  $\sim 200$  pm are occasionally visible, but they exhibit an unusual shape in sawtooth  
6 pattern which symmetry depends on the scanning direction (trace or retrace, not shown). This  
7 indicates a tip-induced structuring of the membrane. A similar effect has previously been reported  
8 on DOPC membrane in specific ionic solutions able to reduce the lipid mobilities.<sup>63</sup> Here these  
9 results suggest that positive potentials help structure the lipid molecules by attracting their  
10 headgroup the membrane, hence limiting their mobility.<sup>63</sup> Dissolved ions do not appear to play a  
11 major role beyond the immediate screening of the charged phosphoserine group. Force-distance  
12 measurements did not show any sizeable rupture force (Supplementary Fig. S5), confirming a  
13 highly fluid membrane. Extensive rinsing of the membrane with ultrapure water revealed  
14 significant structural changes after  $\sim 15$  min equilibration. At 0 V some corrugations  $\sim 150$  pm deep  
15 are already visible and do not depend on the tip scanning direction, suggesting that they represent  
16 an intrinsic properties of the membrane in these conditions. Applying an electric potential of  $\pm 1.0$   
17 V results in corrugations similar in shape and periodicity, but significantly more marked with a  
18 depth often larger than 0.5 nm.  
19  
20  
21  
22  
23  
24  
25  
26  
27  
28  
29  
30  
31  
32  
33  
34  
35  
36  
37  
38  
39

40 The most unusual features are seen in the  $\text{CaCl}_2$  solution where some deep ( $\sim 2$  nm) periodic  
41 corrugations are already apparent at 0 V. Interestingly, while the average periodicity between the  
42 usual row-like features is comparable to that observed in other solution and conditions, the rows  
43 appear grouped three by three, creating higher order corrugations with a periodicity of almost 20  
44 nm. These super-structures appear completely novel and do not match previous reports of hemi-  
45 micellar lipid structures on Au(111).<sup>87-90</sup> The fact that these complex structures develop in  $\text{CaCl}_2$   
46 even in the absence of any applied potential indicate a direct effect of the divalent  $\text{Ca}^{2+}$  ions on the  
47  
48  
49  
50  
51  
52  
53  
54  
55  
56  
57  
58  
59  
60

monolayer structure, presumably through the bridging of multiple lipid headgroups by a single cation.  $\text{Ca}^{2+}$  ions are indeed well known to strongly bind phosphoserine lipids.<sup>91</sup> When a potential of +1.0 V is applied to the HOPG substrate for 15 min, the larger ‘super-corrugations’ remain visible, but the smaller periodicity almost completely vanishes in places. Overall the membrane appears more regular than under open circuit potential. In contrast, applying -1.0 V tends to partially remove the high order super corrugations, but the smaller row-like features appear more clearly with a depth comparable to that visible at 0 V. Altogether, the results with DOPS membranes show that both the ionic solution and the trans-membrane electric potential can affect the lipids molecular assembly, creating some distinctive structural changes. The plausible molecular mechanisms underlying these changes will be detailed in the Discussion section.

**Positively charged lipid membranes** were formed from DOTAP lipid that exhibit cationic trimethylammonium-propane headgroup. As for previous lipids, membranes were examined in the three different ionic solutions and under electrical potentials with representative results shown comparatively in Figure 4. Unlike DOPS membranes, DOTAP membranes exhibit now distinctive features regardless of the imaging conditions, with results reminiscent of images acquired in DOPC (Fig. 2). This is not surprising given the fact that, except for potential hydration effects related to each saline solution,  $\text{Na}^+$  or  $\text{Ca}^{2+}$  cannot adsorb to the TAP headgroup and hence affect the DOTAP assembly. When comparing the solutions, the only difference with direct consequences on the system’s electrostatics is the removal of  $\text{Cl}^-$  ions in ultrapure water where  $\text{OH}^-$  ions are left to ensure electroneutrality. The only voltage-dependent effect visible in the images is a slight increase in apparent membrane roughness in NaCl and water when a positive electric potential is applied, possibly due to a partial repulsion of the DOTAP from the HOPG. The effect is however subtle and the explanation speculative.

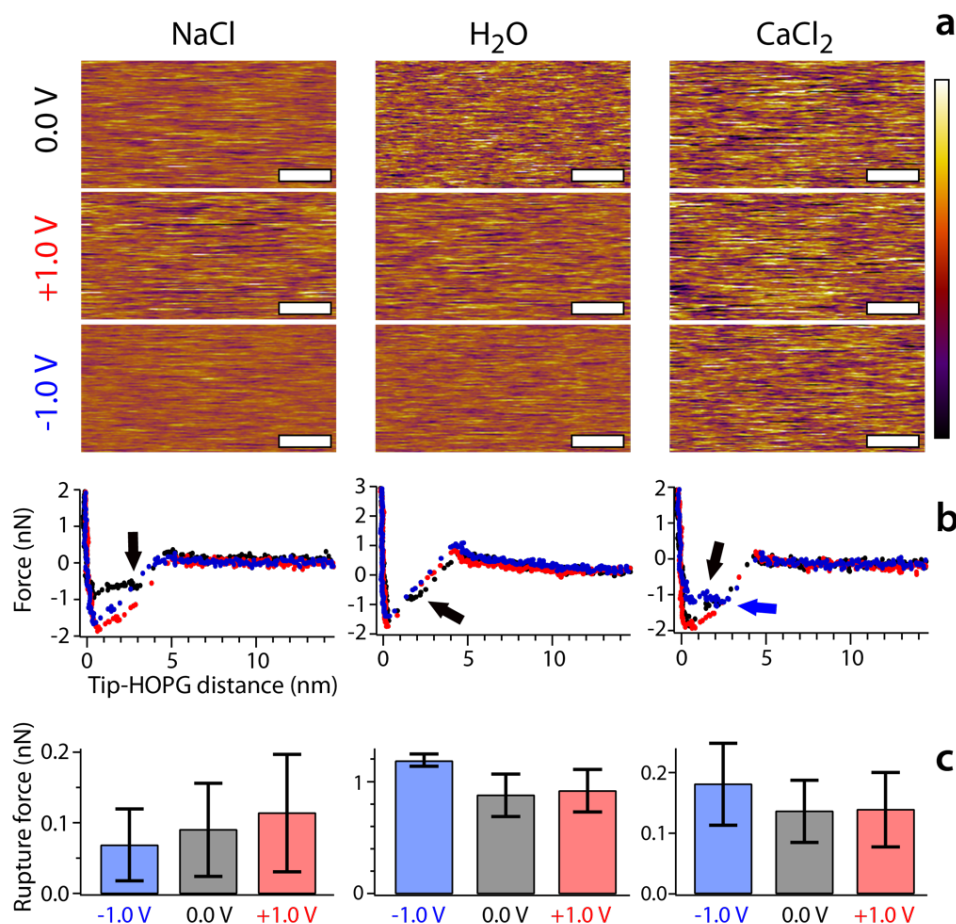


**Figure 4.** Impact of electric potentials on DOTAP monolayers in different ionic solutions. In each solution, a representative topographic image is shown (a) and force distance curve exhibiting membrane rupture (b) is shown for applied potentials of 0 V (black), -1.0 V (blue) and +1.0 V (red). Arrows in (b) indicate sub-steps in the monolayer rupture process. Statistical analysis of >10 force-distance curves reveals the most probable rupture force and its variability in each case (c). The displayed error is twice the width of the Gaussian fit (see Supplementary Fig. S2 for a detailed description of the statistical analysis). Scale bars are 20 nm. The color bar represents 1.8 nm height variation.

More useful information can be derived from a statistical analysis of the membrane rupture force in each condition. In NaCl, the average rupture force is about an order of magnitude lower than in DOPC at all potentials. All the rupture forces are equal within error. Rupture sub-steps are occasionally visible (Fig. 4), suggesting some specific ionic interactions or hydration effects

between the dissolved ions and the TAP headgroups. In contrast, most sub-steps are gone in ultrapure water, except at 0 V. The average rupture force also increases significantly, suggesting that the lack of metal ions rigidifies the membrane. This could be due to direct electrostatic effects: diminished electrostatic screening between headgroups leading to an increased lateral tension within the 2D-confined membrane. However, the fact that the increase in rupture force occurs independently of the applied voltage suggests that direct electrostatic interactions between lipid headgroups does not dominate the membrane cohesion; hydration effects may rather be at play. Consistently, the better electrostatic screening of the lipid headgroups at -1.0 V only marginally increase the observed rupture force with no clear effect within error. In  $\text{CaCl}_2$ , the rupture force decreases again to values about double of those observed in NaCl. Again, the change occurs evenly at all potentials, and rupture-sub steps reappear, consistent with the observations made in NaCl.

**2. Fluorescence recovery after photobleaching (FRAP) measurements**

FRAP measurements were conducted for all lipids in pure water, and in all ionic solutions at different electrical potentials in DOPS. The aim is to complement the AFM measurements and help with the interpretation of AFM results, especially where structural organization of the lipids appear to have a significantly impact. Reference FRAP measurement were conducted on DOPC, DOPS and DOTAP membranes in ultrapure water. The derived lipid mobilities are summarized in table 1. In each case the estimated mobile fraction of the lipids is also given (see Materials and Methods and Supplementary Fig. S6 for more details).

**Table 1.** Lipid mobilities in ultrapure water calculated from FRAP measurements

Lipid	Potential	Mobility ( $\mu\text{m}^2/\text{s}$ )	Mobile fraction (%)
DOPC	-1.0	$0.86 \pm 0.24$	0.75
	0.0	$0.89 \pm 0.15$	0.71
	+1.0	$0.67 \pm 0.24$	0.63
DOPS	-1.0	$1.86 \pm 0.12$	0.90
	0.0	$1.11 \pm 0.21$	0.89
	+1.0	$0.92 \pm 0.25$	0.87
DOTAP	-1.0	$1.06 \pm 0.28$	0.81
	0.0	$1.11 \pm 0.13$	0.88
	+1.0	$1.35 \pm 0.23$	0.86

Both the fluidity and mobile fraction (recovery level) of DOPC are lower than for charged lipids. Interestingly, while AFM experiments show significant corrugations and molecular ordering in DOPS membrane even in pure water, the DOPS mobility is still comparable to that of unstructured DOTAP membranes, and higher than for DOPC. This indicates that the corrugation structure of observed in DOPS represent a dynamical equilibrium with the AFM picking up a time-average structure that still allows for excellent mobility, presumably because of the repulsion between the DOPS and the slightly negatively charged HOPG at open potential. This is also consistent with the low rupture forces measured in DOPS (Fig. S5). The apparent difficulty for DOPC molecules to diffuse freely on HOPG is also consistent with the remarkably large rupture forces observed (Fig. 2), but slightly lower than typical reported DOPC mobilities for bilayers.<sup>92</sup> It is well known that interactions with the supporting solid can locally order the contacting molecules and reduce their diffusion properties,<sup>64, 93-95</sup> including for lipid membranes.<sup>96, 97</sup> Here, the lack of lubrication water between a proximal leaflet and the solid support may be responsible for the lower lipid mobilities. Notwithstanding these details, we note that the lipid mobilities observed on HOPG confirm that

all the lipid membranes remain fluid, and with lipid mobilities comparable to those reported for traditional supported bilayers. This is in itself and success of the approach used here. FRAP measurements in DOPS were conducted in ionic solutions and under applied electrical potentials. The results are summarized in table 2.

**Table 2.** DOPS mobility in ultrapure water calculated from FRAP measurements

Solution	Potential (V)	Mobility ( $\mu\text{m}^2/\text{s}$ )	Mobile fraction (%)
NaCl	-1.0	1.88 $\pm$ 0.12	0.89
	0.0	1.82 $\pm$ 0.17	0.87
	+1.0	1.03 $\pm$ 0.18	0.85
CaCl <sub>2</sub>	-1.0	1.29 $\pm$ 0.26	0.87
	0.0	0.96 $\pm$ 0.24	0.85
	+1.0	0.87 $\pm$ 0.14	0.84

From table 2, it is clear that the mobility of DOPS is the highest in the NaCl solution, followed by ultrapure water and the lowest in CaCl<sub>2</sub>. Electrical potentials appear to have a limited impact on the lipid mobility. This result is fully consistent with the AFM observations (Fig. 3) whereby the more marked the membrane corrugations the lowest the lipid mobility. The fact that the membrane remains fluid in all conditions further supports the hypothesis that the AFM captures the time average of a dynamical molecular arrangement where lipid molecules remain mobile. The mobilities are, however, affected by the ionic environment suggesting that while the membranes remain fluid, environments inducing significant structural organization of the membrane will also reduce the lipid mobility. This result is similar to that reported recently by Piantanida et al. for DOPC bilayers on a hydrophilic substrate,<sup>63</sup> demonstrating that the generality of ionic effects in modulating lipid membranes' mesoscale organization and mobility. The supporting solid has an

influence on the equilibrium structures formed with here longitudinal row consistent with the crystalline lattice of the HOPG. However, it is the ions that primarily drive the clustering on lipid molecules, rendering the formation of structures possible in the first place.

## General Discussion

The AFM results and the FRAP measurements both show that HOPG is able to support fluid lipid monolayers, with properties and mobilities close to those of standard supported lipid bilayers at rest (no potential).<sup>92</sup> When an electrical potential is applied, the monolayers can form some mesoscale molecular arrangements (corrugations) depending on the nature of the lipids, the ionic environment and applied trans-membrane electric fields. Similar results have previously been reported for bilayers on metal electrodes,<sup>18</sup> again supporting HOPG as a suitable substrate for studying electrochemical effects occurring at the interface between lipid membranes and aqueous solutions.

Significantly, the results demonstrate that ionic effects dominate over electrical fields within the range of potentials investigated here, with membrane rupture forces and patterns suggesting that field to act as a fine tuning of the lipids molecular arrangement. The electrical potential is also able to modulate the concentration of dissolved ions at the membrane-solution interface and hence indirectly influence the ionic effects.

While DOPC and DOTAP membranes remain globally unstructured in most solutions and under potentials, DOPS membranes exhibit striking features that indicate a significant degree of mesoscale lipid ordering. Fig. 5 proposes a model of the molecular mechanisms responsible for the features reported in Fig. 3. In NaCl (membrane deposition solution), the Na<sup>+</sup> ions ensure electroneutrality of the headgroup (Fig. 5, NaCl). Shallow corrugations are visible when +1.0 V is

applied, presumably due to attraction of  $\text{Cl}^-$  anions at the membrane-solution interface, thereby disrupting the existing hydration structure. Direct electrostatic attraction between the phosphoserine headgroups and the HOPG may also play a role. Consistently, no corrugations are seen at  $-1.0\text{ V}$ . Subsequent rinsing with ultrapure water upset the hydration structure of the membrane and its electrostatic balance, changing the lipid arrangement in the membrane. In the absence of potential, the DOPS forms a hemimicelle-like arrangement reminiscent of detergents on HOPG.<sup>98-100</sup> Applying electrical potential exacerbates the apparent amplitude of the corrugations but not their overall shape, suggesting a subtle effect involving water molecular and the lipid headgroups since electrostatics alone cannot explain the symmetry between  $\pm 1.0\text{ V}$  (Fig.5,  $\text{H}_2\text{O}$ ).

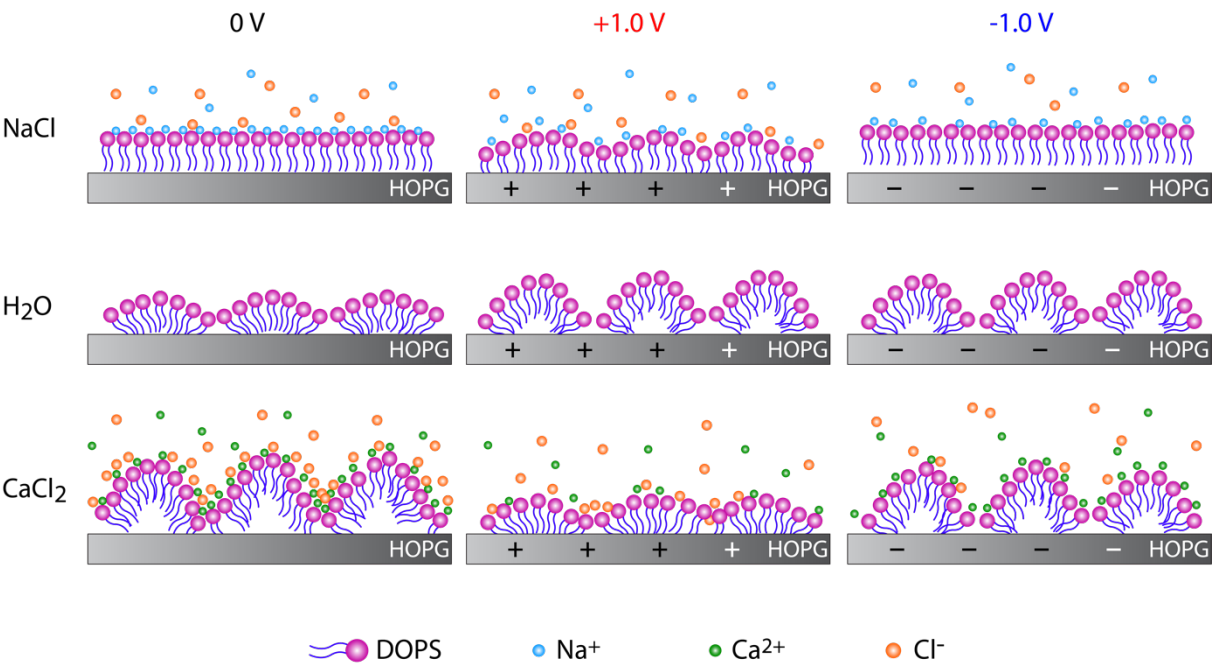


**Figure 5.** Schematic representation of the molecular organization of a DOPS monolayer on HOPG in different ionic environments and under electrical potentials. Not to scale.



1  
2  
3 However, the increased lipid mobility at -1.0 V still suggests a global repulsion between the  
4 headgroups and the HOPG surface. Rinsing of the membrane with  $\text{CaCl}_2$  solution led to larger  
5 corrugations (Fig. 5,  $\text{CaCl}_2$ ) with a clear and distinct impact of applied potentials. The spontaneous  
6 curvature at 0 V and the different response to positive and negative potentials all point to  $\text{Ca}^{2+}$  ions  
7 dominating the system through specific interactions with the lipid headgroups. When +1.0 V is  
8 applied, partial desorption of  $\text{Ca}^{2+}$  cations blurs out the corrugations while at -1.0 V the structures  
9 are reinforced, presumably due to a locally increased  $\text{Ca}^{2+}$  concentration. It is well known that  
10 electrically-induced adsorption of ions in monolayers can influence the membrane phase  
11 transition<sup>58</sup> depending on the magnitude and sign of the potential.<sup>57</sup>

22 We note that the silicon oxide AFM tip is negatively charged in all the experimental conditions  
23 examined in this study. This negative surface potential can in principle impact the AFM  
24 measurements, in particular those of rupture forces. This effect is unlikely to appreciably affect  
25 the measurements in ionic solutions due to electrostatic screening of the tip by the dissolved ions.  
26 In ultrapure water, electrostatic tip effects on the measured rupture forces can *a priori* not be  
27 excluded, for example with DOPC and DOTAP membranes. Direct electrostatic interactions  
28 between the tip and the HOPG may also be at play. However, hydration effects appear to dominate  
29 of direct electrostatics and the applied potentials tend not to provide consistent differences with  
30 open circuit rupture forces. Additionally, the voltages imposed here are more than an order of  
31 magnitude larger than the surface potential of the tip suggesting that tip effects can be seen as a  
32 small perturbation of the system. We also note the consistency of the FRAP measurements with  
33 the AFM results suggesting the latter to be reliable, at least with respect to the reported trends.

**Conclusions**

In this work we investigate the nanoscale structure and dynamics of HOPG-supported phospholipid monolayers in different ionic solutions and under electrical potential. Combining AFM in liquid with FRAP measurements, we show that ions can induce mesoscale ordered molecular structures within the lipid membrane while retaining its fluidity. Experiments in NaCl, CaCl<sub>2</sub> and ultrapure water suggest that these effects are dominated by ion-mediated hydration forces with direct electrostatic interactions playing a secondary role while still present. Electric fields can influence the molecular organization, cohesion and dynamics of the lipids in the membrane, but not as dramatically as ions and in particular calcium, at least for the voltages explored here ( $\pm 1.0$  V). The results strongly depend on the type of lipid considered, with particularly marked effects in DOPS. In comparison, zwitterionic and cationic lipid showed little or no ordering effect aside from changes in the membrane rupture force. While the present study does not control the actual trans-membrane potential, experiments imposing smaller voltages (400 mV) induced very similar membrane changes and molecular rearrangements, but requiring a longer equilibration time, consistently with previous studies.<sup>90, 101</sup> Natural trans-membrane potentials in biology typically have a comparable magnitude, ranging over few hundreds of millivolts. This suggests our results to be of relevance for natural biological system where trans-membrane potential may help control the lipid molecular arrangement and the membrane permeability. We believe our findings could have significant implications in the development of lab-on chip lipid-based devices, and for understanding the effect trans-membrane potentials on the molecular ordering of lipids in biological membranes, in particular with view of mimicking biological electrochemical function.

## ASSOCIATED CONTENT

### Supporting Information

The following file is available free of charge. Preparation procedures for the Ag/AgCl electrode, electrochemical impedance spectroscopy results, description of the procedure used to analyze the AFM spectroscopy, example of rupture forces recorded for DOPS in NaCl solution, and representative FRAP experiments of lipids (Figures S1-S6) (PDF)

## AUTHOR INFORMATION

### Corresponding Author

\*E-mail: [hanxiaojun@hit.edu.cn](mailto:hanxiaojun@hit.edu.cn)

\*E-mail: [kislon.voitchovsky@durham.ac.uk](mailto:kislon.voitchovsky@durham.ac.uk)

### Author Contributions

Hongmei Bi, Xiaojun Han and KislonoVoitchovsky conceived the study and designed the experiments. Hongmei Bi conducted the measurements. Xuejing Wang supplemented some FRAP experiments. KislonoVoitchovsky analyzed the AFM data. Hongmei Bi wrote the manuscript; Xiaojun Han and KislonoVoitchovsky revised the manuscript.

### Notes

The authors declare no competing financial interest.

## ACKNOWLEDGMENTS

We thank William Trewby (Durham) for help with AFM measurement and Ethan J. Miller (Durham) for his assistance in the FRAP experiments. This research was supported by the National Natural Science Foundation of China (Grant No. 21503072, 21773050), Program of Introduction Talents in University (Grant No. XDB-2017-19), and sponsored by China Scholarship Council (Grant No. 20163035). KV acknowledges financial support from the Royal Society International Exchange program (IE140921), the Engineering and Physical Sciences Research Council (EP/M023915/1) and the European Council (MC CIG 631186).

## REFERENCES

- (1) Pignatello, R., Biological Membranes and Their Role in Physio-pathological Conditions. In Drug-Biomembrane Interaction Studies: The Application of Calorimetric Techniques, Pignatello, R., Ed. *Woodhead Publ Ltd: Cambridge*, **2013**; pp 1-46.
- (2) Orsini, F.; Migliaccio, E.; Moroni, M.; Contursi, C.; Raker, V. A.; Piccini, D.; Martin-Padura, I.; Pelliccia, G.; Trinei, M.; Bono, M.; Puri, C.; Tacchetti, C.; Ferrini, M.; Mannucci, R.; Nicoletti, I.; Lanfranccone, L.; Giorgio, M.; Pelicci, P. G., The Life Span Determinant P66Shc Localizes to Mitochondria Where it Associates with Mitochondrial Heat Shock Protein 70 and Regulates Trans-membrane Potential. *J. Biol. Chem*, **2004**, *279*, (24), 25689-25695.
- (3) Strahl, H.; Hamoen, L. W., Membrane Potential is Important for Bacterial Cell Division. *Proc. Natl. Acad. Sci. U.S.A.* **2010**, *107*, (27), 12281-12286.
- (4) Yu, H.; Yzeiri, I.; Hou, B. Y.; Chen, C. H.; Bu, W.; Vanysek, P.; Chen, Y. S.; Lin, B. H.; Kral, P.; Schlossman, M. L., Electric Field Effect on Phospholipid Monolayers at an Aqueous-Organic Liquid-Liquid Interface. *J. Phys. Chem. B*, **2015**, *119*, (29), 9319-9334.

- (5) Cheetham, M. R.; Bramble, J. P.; McMillan, D. G.; Krzeminski, L.; Han, X.; Johnson, B. R.; Bushby, R. J.; Olmsted, P. D.; Jeuken, L. J.; Marritt, S. J.; Butt, J. N.; Evans, S. D., Concentrating Membrane Proteins using Asymmetric Traps and AC Electric Fields. *J. Am. Chem. Soc.*, **2011**, *133*, (17), 6521-6524.
- (6) Jonsson, P.; Beech, J. P.; Tegenfeldt, J. O.; Hook, F., Mechanical Behavior of a Supported Lipid Bilayer under External Shear Forces. *Langmuir*, **2009**, *25*, (11), 6279-6286.
- (7) Jonsson, P.; Gunnarsson, A.; Hook, F., Accumulation and Separation of Membrane-Bound Proteins using Hydrodynamic Forces. *J. Am. Chem. Soc.*, **2011**, *83*, (2), 604-611.
- (8) Han, X.; Cheetham, M. R.; Sheikh, K.; Olmsted, P. D.; Bushby, R. J.; Evans, S. D., Manipulation and Charge Determination of Proteins in Photopatterned Solid Supported Bilayers. *Integrative biology*, **2009**, *1*, (2), 205-211.
- (9) Groves, J. T.; Boxer, S. G., Micropattern Formation in Supported Lipid Membranes. *Accounts. Chem. Res.*, **2002**, *35*, (3), 149-157.
- (10) Roth, J. S.; Zhang, Y.; Bao, P.; Cheetham, M. R.; Han, X.; Evans, S. D., Optimization of Brownian Ratchets for the Manipulation of Charged Components within Supported Lipid Bilayers. *Appl. Phys. Lett.*, **2015**, *106*, (18).
- (11) Pluhackova, K.; Bockmann, R. A., Biomembranes in Atomistic and Coarse-grained Simulations. *J. Phys. Condens. Matter*, **2015**, *27*, (32), 19.
- (12) Fuentes, N. R.; Salinas, M. L.; Kim, E.; Chapkin, R. S., Emerging Role of Chemoprotective Agents Plasma Membrane Organization. *BBA-Biomembranes*, **2017**, *1859*, (9), 1668-1678.
- (13) Voitchovsky, K.; Contera, S. A.; Kamihira, M.; Watts, A.; Ryan, J. F., Differential stiffness and lipid mobility in the leaflets of purple membranes. *Biophys. J.* **2006**, *90*, (6), 2075-2085.

- (14) Contera, S. A.; Voitchovsky, K.; Ryan, J. F., Controlled ionic condensation at the surface of a native extremophile membrane. *Nanoscale*, **2010**, 2, (2), 222-229.
- (15) Voitchovsky, K.; Contera, S. A.; Ryan, J. F., Electrostatic and steric interactions determine bacteriorhodopsin single-molecule biomechanics. *Biophys. J.* **2007**, 93, (6), 2024-2037.
- (16) Bao, P.; Cartron, M. L.; Sheikh, K. H.; Johnson, B. R. G.; Hunter, C. N.; Evans, S. D., Controlling Transmembrane Protein Concentration and Orientation in Supported Lipid Bilayers. *Chem. Commun.*, **2017**, 53 (30), 4250-4253.
- (17) Akbari, E.; Buntat, Z.; Shahraki, E.; Parvaz, R.; Kiani, M. J., Analytical Investigation of Bilayer Lipid Biosensor Based on Graphene. *J. Biomater. Appl.*, **2016**, 30, (6), 677-685.
- (18) Staffa, J. K.; Lorenz, L.; Stolarski, M.; Murgida, D. H.; Zebger, I.; Utesch, T.; Kozuch, J.; Hildebrandt, P., Determination of the Local Electric Field at Au/SAM Interfaces Using the Vibrational Stark Effect. *J. Phys. Chem. C*, **2017**, 121, (40), 22274-22285.
- (19) Madrid, E.; Horswell, S. L., Effect of Electric Field on Structure and Dynamics of Bilayers Formed From Anionic Phospholipids. *Electrochim. Acta*, **2014**, 146, 850-860.
- (20) Kuo, C. K.; Hochstrasser, R. M., Super-resolution Microscopy of Lipid Bilayer Phases. *J. Am. Chem. Soc.*, **2011**, 133, (13), 4664-4667.
- (21) Chen, M. H.; Li, M.; Brosseau, C. L.; Lipkowski, J., AFM Studies of the Effect of Temperature and Electric Field on the Structure of a DMPC-Cholesterol Bilayer Supported on a Au(111) Electrode Surface. *Langmuir*, **2009**, 25, (2), 1028-1037.
- (22) Jeuken, L. J. C., AFM Study on the Electric-field Effects on Supported Bilayer Lipid Membranes. *Biophys. J.*, **2008**, 94, (12), 4711-4717.
- (23) Li, J. K.; Sullan, R. M. A.; Zou, S., Atomic Force Microscopy Force Mapping in the Study of Supported Lipid Bilayers. *Langmuir*, **2011**, 27, (4), 1308-1313.

- (24) Yuan, J.; Hao, C. C.; Chen, M. H.; Berini, P.; Zou, S., Lipid Reassembly in Asymmetric Langmuir-Blodgett/Langmuir-Schaeffer Bilayers. *Langmuir*, **2013**, *29*, (1), 221-227.
- (25) Bhojoo, U.; Chen, M. H.; Zou, S., Temperature induced lipid membrane restructuring and changes in nanomechanics. *Biochim. Biophys. Acta-Biomembranes*, **2018**, *1860*, (3), 700-709.
- (26) Goksu, E. I.; Vanegas, J. M.; Blanchette, C. D.; Lin, W. C.; Longo, M. L., AFM for Structure and Dynamics of Biomembranes. *Biochim. Biophys. Acta -Biomembranes*, **2009**, *1788*, (1), 254-266.
- (27) Lebegue, E.; Smida, H.; Flinois, T.; Vie, V.; Lagrost, C.; Barriere, F., An Optimal Surface Concentration of Pure Cardiolipin Deposited onto Glassy Carbon Electrode Promoting the Direct Electron Transfer of Cytochrome-c. *J. Electroanal. Chem.*, **2018**, *808*, 286-292.
- (28) Abbasi, F.; Leitch, J. J.; Su, Z. F.; Szymanski, G.; Lipkowski, J., Direct Visualization of Alamethicin Ion Pores Formed in a Floating Phospholipid Membrane Supported on a Gold Electrode surface. *Electrochim. Acta*, **2018**, *267*, 195-205.
- (29) Juhaniewicz, J.; Sek, S., Atomic Force Microscopy and Electrochemical Studies of Melittin Action on Lipid Bilayers Supported on Gold Electrodes. *Electrochim. Acta*, **2015**, *162*, 53-61.
- (30) Cannes, C.; Kanoufi, F.; Bard, A. J., Cyclic Voltammetry and Scanning Electrochemical Microscopy of Ferrocenemethanol at Monolayer and Bilayer-modified Gold Electrodes. *J. Electroanal. Chem*, **2003**, *547*, (1), 83-91.
- (31) Zawisza, I.; Bin, X. M.; Lipkowski, J., Spectroelectrochemical Studies of Bilayers of Phospholipids in Gel and Liquid State on Au(111) Electrode Surface. *Bioelectrochemistry*, **2004**, *63*, (1-2), 137-147.

- (32) Burgess, I.; Li, M.; Horswell, S. L.; Szymanski, G.; Lipkowski, J.; Majewski, J.; Satija, S., Electric Field-driven Transformations of a Supported Model Biological Membrane - An Electrochemical and Neutron Reflectivity Study. *Biophys. J.*, **2004**, *86*, (3), 1763-1776.
- (33) Lipkowski, J., Building Biomimetic Membrane at a Gold Electrode Surface. *Phys. Chem. Chem. Phys.*, **2010**, *12*, (42), 13874-13887.
- (34) Burgess, I.; Li, M.; Horswell, S. L.; Szymanski, G.; Lipkowski, J.; Satija, S.; Majewski, J., Influence of the Electric Field on a Bio-mimetic Film Supported on a Gold Electrode. *Colloid. Surface. B*, **2005**, *40*, (3-4), 117-122.
- (35) Krysinski, P.; Moncelli, M. R.; Tadini-Buoninsegni, F., A Voltammetric Study of Monolayers and Bilayers Self-assembled on Metal Electrodes. *Electrochim. Acta*, **2000**, *45*, (12), 1885-1892.
- (36) Li, M.; Chen, M.; Sheepwash, E.; Brosseau, C. L.; Li, H.; Pettinger, B.; Gruler, H.; Lipkowski, J., AFM Studies of Solid-supported Lipid Bilayers Formed at a Au(111) Electrode Surface using Vesicle Fusion and a Combination of Langmuir-Blodgett and Langmuir-Schaefer Techniques. *Langmuir*, **2008**, *24*, (18), 10313-10323.
- (37) Kycia, A. H.; Wang, J. P.; Merrill, A. R.; Lipkowski, J., Atomic Force Microscopy Studies of a Floating-Bilayer Lipid Membrane on a Au(111) Surface Modified with a Hydrophilic Monolayer. *Langmuir*, **2011**, *27*, (17), 10867-10877.
- (38) Donaldson, S. H.; Valtiner, M.; Gebbie, M. A.; Haradad, J.; Israelachvili, J. N., Interactions and Visualization of Bio-mimetic Membrane Detachment at Smooth and Nano-rough Gold Electrode Surfaces. *Soft Matter*, **2013**, *9*, (21), 5231-5238.



- (39) Matyszewska, D.; Sek, S.; Jablonowska, E.; Palys, B.; Pawlowski, J.; Bilewicz, R.; Konrad, F.; Osornio, Y. M.; Landau, E. M., Dependence of Interfacial Film Organization on Lipid Molecular Structure. *Langmuir*, **2014**, *30*, (38), 11329-11339.
- (40) Gutierrez-Sanchez, C.; Olea, D.; Marques, M.; Fernandez, V. M.; Pereira, I. A. C.; Velez, M.; De Lacey, A. L., Oriented Immobilization of a Membrane-Bound Hydrogenase onto an Electrode for Direct Electron Transfer. *Langmuir*, **2011**, *27*, (10), 6449-6457.
- (41) Marques, J. T.; de Almeida, R. F. M.; Viana, A. S., Biomimetic Membrane Rafts Stably Supported on Unmodified Gold. *Soft Matter*, **2012**, *8*, (6), 2007-2016.
- (42) Ip, S.; Li, J. K.; Walker, G. C., Phase Segregation of Untethered Zwitterionic Model Lipid Bilayers Observed on Mercaptoundecanoic-Acid-Modified Gold by AFM Imaging. *Langmuir*, **2010**, *26*, (13), 11060-11070.
- (43) Kocábová, J.; Kolivoška, V.; Gál, M.; Sokolová, R., Tuning phospholipid bilayer permeability by flavonoid apigenin: Electrochemical and atomic force microscopy study. *J. Electroanal. Chem.*, **2018**, *821*, 67-72.
- (44) Brukhno, A. V.; Akinshina, A.; Coldrick, Z.; Nelson, A.; Auer, S., Phase Phenomena in Supported Lipid Films under Varying Electric Potential. *Soft Matter*, **2011**, *7*, (3), 1006-1017.
- (45) Leermakers, F. A. M.; Nelson, A., Substrate-induced Structural-changes in Electrode-adsorbed Lipid Layers-self Consistent Field-theory. *J. Electroanal. Chem*, **1990**, *278*, (1-2), 53-72.
- (46) Nelson, A.; Leermakers, F. A. M., Substrate-induced Structural-changes in Electrode-adsorbed Lipid Layers-experimental- Evidence from the Behavior of Phospholipid Layers on the Mercury Water Interface. *J. Electroanal. Chem*, **1990**, *278*, (1-2), 73-83.

- (47) Monne, J.; Diez, Y.; Puy, J.; Galceran, J.; Nelson, A., Interpreting Ion Fluxes to Channel Arrays in Monolayers. *Langmuir*, **2007**, *23*, (21), 10581-10588.
- (48) Nelson, A., Conducting Gramicidin Channel Activity in Phospholipid Monolayers. *Biophys. J.*, **2001**, *80*, (6), 2694-2703.
- (49) Nelson, A., Electrochemistry of Mercury Supported Phospholipid Monolayers and Bilayers. *Curr. Opin. Colloid. Interf.*, **2010**, *15*, (6), 455-466.
- (50) Whitehouse, C.; O'Flanagan, R.; Lindholm-Sethson, B.; Movaghar, B.; Nelson, A., Application of Electrochemical Impedance Spectroscopy to the Study of Dioleoyl Phosphatidylcholine Monolayers on Mercury. *Langmuir*, **2004**, *20*, (1), 136-144.
- (51) Bizzotto, D.; Yang, Y. G.; Shepherd, J. L.; Stoodley, R.; Agak, J.; Stauffer, V.; Lathuilliere, M.; Akhtar, A. S.; Chung, E., Electrochemical and Spectroelectrochemical Characterization of Lipid Organization in an Electric Field. *J. Electroanal. Chem.*, **2004**, *574*, (1), 167-184.
- (52) Gao, X. P.; White, H. S.; Chen, S. W.; Abruna, H. D., Electric-Field-Induced Transition of Amphiphilic Layers on Mercury-Electrodes. *Langmuir*, **1995**, *11*, (11), 4554-4563.
- (53) Herrero, R.; Barriada, J. L.; Lopez-Fonseca, J. M.; Moncelli, M. R.; de Vicente, M. E. S., Effect of Ionic Strength on the Electrochemical Behavior of Glutathione on a Phospholipid Self-Assembled Monolayer on Mercury. *Langmuir*, **2000**, *16*, (11), 5148-5153.
- (54) Mauzeroll, J.; Buda, M.; Bard, A. J.; Prieto, F.; Rueda, M., Detection of Tl(I) Transport through a Gramicidin-dioleoylphosphatidylcholine Monolayer using the Substrate Generation-tip Collection Mode of Scanning Electrochemical Microscopy. *Langmuir*, **2002**, *18*, (24), 9453-9461.
- (55) Coldrick, Z.; Steenson, P.; Millner, P.; Davies, M.; Nelson, A., Phospholipid Monolayer Coated Microfabricated Electrodes to Model the Interaction of Molecules with Biomembranes. *Electrochim. Acta*, **2009**, *54*, (22), 4954-4962.

- (56) Coldrick, Z.; Penezic, A.; Gasparovic, B.; Steenson, P.; Merrifield, J.; Nelson, A., High Throughput Systems for Screening Biomembrane Interactions on Fabricated Mercury Film Electrodes. *J. Appl. Electrochem*, **2011**, *41*, (8), 939-949.
- (57) Nelson, A., Electrochemical Analysis of APhospholipid Phase Transition. *J. Electroanal. Chem*, **2007**, *601*, (1-2), 83-93.
- (58) Vakurov, A.; Galluzzi, M.; Podesta, A.; Gamper, N.; Nelson, A. L.; Connell, S. D. A., Direct Characterization of Fluid Lipid Assemblies on Mercury in Electric Fields. *ACS Nano*, **2014**, *8*, (4), 3242-3250.
- (59) Stoodley, R.; Bizzotto, D., Epi-fluorescence Microscopic Characterization of Potential-Induced Changes in a DOPC Monolayer on a Hg Drop. *Analyst*, **2003**, *128*, (6), 552-561.
- (60) Mustata, G. M.; Kim, Y. H.; Zhang, J.; DeGrado, W. F.; Grigoryan, G.; Wanunu, M., Graphene Symmetry Amplified by Designed Peptide Self-Assembly. *Biophys. J.*, **2016**, *110*, (11), 2507-2516.
- (61) Hayamizu, Y.; So, C. R.; Dag, S.; Page, T. S.; Starkebaum, D.; Sarikaya, M., Bioelectronic Interfaces by Spontaneously Organized Peptides on 2D Atomic Single Layer Materials. *Sci. Rep.*, **2016**, *6*, 33778.
- (62) Seki, T.; So, C. R.; Page, T. R.; Starkebaum, D.; Hayamizu, Y.; Sarikaya, M., Electrochemical Control of Peptide Self-Organization on Atomically Flat Solid Surfaces: A Case Study with Graphite. *Langmuir*, **2017**, *34*, 1819-1826.
- (63) Piantanida, L.; Bolt, H. L.; Rozatian, N.; Cobb, S. L.; Voitchovsky, K., Ions Modulate Stress-Induced Nanotexture in Supported Fluid Lipid Bilayers. *Biophys. J.*, **2017**, *113*, (2), 426-439.

- (64) Voitchovsky, K.; Giofre, D.; Segura, J. J.; Stellacci, F.; Ceriotti, M., Thermally-nucleated Self-assembly of Water and Alcohol into Stable Structures at Hydrophobic Interfaces. *Nat. Commun.*, **2016**, *7*, 13064.
- (65) Ricci, M.; Quinlan, R. A.; Voitchovsky, K., Sub-nanometre Mapping of the Aquaporin-Water Interface using Multifrequency Atomic Force Microscopy. *Soft Matter*, **2017**, *13*, (1), 187-195.
- (66) Ricci, M.; Trewby, W.; Cafolla, C.; Voitchovsky, K., Direct Observation of the Dynamics of Single Metal ions at the Interface with Solids in Aqueous Solutions. *Sci. Rep.*, **2017**, *7*, 43234.
- (67) Trewby, W.; Livesey, D.; Voitchovsky, K., Buffering Agents Modify the Hydration Landscape at Charged Interfaces. *Soft Matter*, **2016**, *12*, (9), 2642-2651.
- (68) Mingeot-Leclercq, M. P.; Deleu, M.; Brasseur, R.; Dufrene, Y. F., Atomic Force Microscopy of Supported Lipid Bilayers. *Nat. Protoc.*, **2008**, *3*, (10), 1654-1659.
- (69) Richter, R. P.; Berat, R.; Brisson, A. R., Formation of Solid-supported Lipid Bilayers: an Integrated View. *Langmuir*, **2006**, *22*, (8), 3497-505.
- (70) Wang, X. J.; Zhang, Y.; Bi, H. M.; Han, X. J., Supported Lipid Bilayer Membrane Arrays on Micro-patterned ITO Electrodes. *RSC Adv*, **2016**, *6*, (76), 72821-72826.
- (71) Miller, E. J.; Trewby, W.; Payam, A. F.; Piantanida, L.; Cafolla, C.; Voitchovsky, K., Sub-nanometer Resolution Imaging with Amplitude-modulation Atomic Force Microscopy in Liquid. *J. Vis. Exp.* **2016**, *118*, e54924.
- (72) Voitchovsky, K., Anharmonicity, solvation forces, and resolution in atomic force microscopy at the solid-liquid interface. *Phys. Rev. E*, **2013**, *88*, (2), 022407.
- (73) Schneider, C. A.; Rasband, W. S.; Eliceiri, K. W., NIH Image to ImageJ: 25 Years of Image Analysis. *Nat. Methods*, **2012**, *9*, (7), 671-675.

- (74) Soumpasis, D. M., Theoretical Analysis of Fluorescence Photobleaching Recovery Experiments. *Biophys. J.*, **1983**, *41*, (1), 95-97.
- (75) McKiernan, A. E.; Ratto, T. V.; Longo, M. L., Domain Growth, Shapes, and Topology in Cationic Lipid Bilayers on Mica by Fluorescence and Atomic Force Microscopy. *Biophys. J.*, **2000**, *79*, (5), 2605-2615.
- (76) Kang, M.; Day, C. A.; Kenworthy, A. K.; DiBenedetto, E., Simplified Equation to Extract Diffusion Coefficients from Confocal FRAP Data. *Traffic*, **2012**, *13*, (12), 1589-1600.
- (77) Blumenthal, D.; Goldstien, L.; Edidin, M.; Gheber, L. A., Universal Approach to FRAP Analysis of Arbitrary Bleaching Patterns. *Sci. Rep.*, **2015**, *5*, 11655.
- (78) Zawisza, I.; Bin, X. M.; Lipkowski, J., Potential-driven structural changes in Langmuir-Blodgett DMPC bilayers determined by in situ spectroelectrochemical PM IRRAS. *Langmuir*, **2007**, *23*, 5180-5194
- (79) Wang, B.; Zhang, L. F.; Bae, S. C.; Granick, S., Nanoparticle-induced Surface Reconstruction of Phospholipid Membranes. *Proc. Natl. Acad. Sci. U.S.A.* **2008**, *105*, (47), 18171-18175.
- (80) Guriyanova, S.; Mairanovsky, V. G.; Bonaccorso, E., Superviscosity and Electroviscous Effects at an Electrode/aqueous Electrolyte Interface: An Atomic Force Microscope Study. *J. Colloid. Inter. Sci.*, **2011**, *360*, (2), 800-804.
- (81) Wang, J. J.; Li, T. L.; Bateman, S. D.; Erck, R.; Morris, K. R., Modeling of Adhesion in Tablet Compression - I. Atomic Force Microscopy and Molecular Simulation. *J. Pharm. Sci.*, **2003**, *92*, (4), 798-814.

- (82) Obst, M.; Dittrich, M.; Kuehn, H., Calcium Adsorption and Changes of the Surface Microtopography of Cyanobacteria Studied by AFM, CFM, and TEM with Respect to Biogenic Calcite Nucleation. *Geochem. Geophys. Geosy.* **2006**, *7*.
- (83) Peng, H.; Birkett, G. R.; Nguyen, A. V., Origin of Interfacial Nanoscopic Gaseous Domains and Formation of Dense Gas Layer at Hydrophobic Solid-Water Interface. *Langmuir*, **2013**, *29*, (49), 15266-15274.
- (84) Lenz, P.; Ajo-Franklin, C. M.; Boxer, S. G., Patterned Supported Lipid Bilayers and Monolayers on Poly (dimethylsiloxane). *Langmuir*, **2004**, *20*, (25), 11092-11099.
- (85) Montal, M.; Mueller, P., Formation of bimolecular membranes from lipid monolayers and a study of their electrical properties. *Proc. Natl. Acad. Sci. U.S.A.* **1972**, *69*, (12), 3561-3566.
- (86) Romer, W.; Steinem, C., Impedance analysis and single-channel recordings on nano-black lipid membranes based on porous alumina. *Biophys. J.* **2004**, *86*, (2), 955-965.
- (87) Xu, S. M.; Szymanski, G.; Lipkowski, J., Self-assembly of phospholipid molecules at a Au(111) electrode surface. *J. Am. Chem. Soc.* **2004**, *126*, (39), 12276-12277.
- (88) Petri, M.; Kolb, D. M., Nanostructuring of a sodium dodecyl sulfate-covered Au(111) electrode. *Phys. Chem. Chem. Phys.* **2002**, *4*, (7), 1211-1216.
- (89) Pawlowski, J.; Juhaniewicz, J.; Guzeloglu, A.; Sek, S., Mechanism of Lipid Vesicles Spreading and Bilayer Formation on a Au(111) Surface. *Langmuir*, **2015**, *31*, (40), 11012-11019.
- (90) Matsunaga, S.; Shimizu, H.; Yamada, T.; Kobayashi, T.; Kawai, M., In Situ STM and Vibrational Study of Nanometer-Scale Reorganization of a Phospholipid Monolayer Accompanied by Potential-Driven Headgroup Digestion. *Langmuir*, **2017**, *33*, (46), 13157-13167.
- (91) Casal, H. L.; Mantsch, H. H.; Hauser, H., Infrared studies of fully hydrated saturated phosphatidylserine Bilayers - effect of  $\text{Li}^+$  and  $\text{Ca}^{2+}$ . *Biochemistry*, **1987**, *26*, 4408-4416.

- (92) Zhang, Y.; Wang, X. J.; Ma, S. H.; Jiang, K. P.; Han, X. J., Lipid Membrane Formation on Chemical Gradient Modified Surfaces. *RSC Adv.*, **2016**, *6*, (14), 11325-11328.
- (93) Sedlmeier, F.; von Hansen, Y.; Mengyu, L.; Horinek, D.; Netz, R. R., Water Dynamics at Interfaces and Solutes: Disentangling Free Energy and Diffusivity Contributions. *J. Stat. Phys.*, **2011**, *145*, (2), 240-252.
- (94) Toppozini, L.; Roosen-Runge, F.; Bewley, R. I.; Dalglish, R. M.; Perring, T.; Seydel, T.; Glyde, H. R.; Sakai, V. G.; Rheinstadter, M. C., Anomalous and Anisotropic Nanoscale Diffusion of Hydration Water Molecules in Fluid Lipid Membranes. *Soft Matter*, **2015**, *11*, (42), 8354-8371.
- (95) Von Hansen, Y.; Gekle, S.; Netz, R. R., Anomalous Anisotropic Diffusion Dynamics of Hydration Water at Lipid Membranes. *Phys. Rev. Lett.*, **2013**, *111*, 118103.
- (96) Charrier, A.; Thibaudau, F., Main Phase Transitions in Supported Lipid Single-bilayer. *Biophys. J.*, **2005**, *89*, (2), 1094-1101.
- (97) Alessandrini, A.; Seeger, H. M.; Di Cerbo, A.; Caramaschi, T.; Facci, P., What do We Really Measure in AFM Punch-through Experiments on Supported Lipid Bilayers? *Soft Matter*, **2011**, *7*, (15), 7054-7064.
- (98) Yesylevskyy, S. O.; Ramseyer, C., Determination of Mean and Gaussian Curvatures of Highly Curved Asymmetric Lipid Bilayers: the Case Study of the Influence of Cholesterol on the Membrane Shape. *Phys. Chem. Chem. Phys.*, **2014**, *16*, (32), 17052-17061.
- (99) Frotscher, E.; Danielczak, B.; Vargas, C.; Meister, A.; Durand, G.; Keller, S., A Fluorinated Detergent for Membrane-Protein Applications. *Angew. Chem. Intl.*, **2015**, *54*, (17), 5069-5073.
- (100) Grison, M. S.; Brocard, L.; Fouillen, L.; Nicolas, W.; Wewer, V.; Dormann, P.; Nacir, H.; Benitez-Alfonso, Y.; Claverol, S.; Germain, V.; Boutte, Y.; Mongrand, S.; Bayer, E. M., Specific

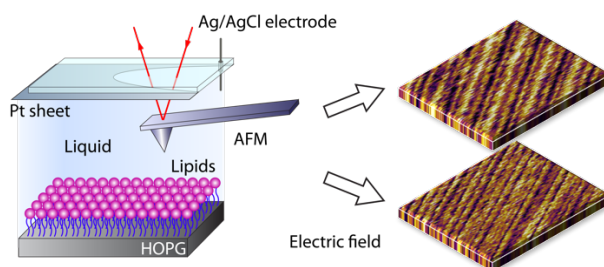
1  
2  
3  
4  
5  
6  
7  
8  
9  
10  
11  
12  
13  
14  
15  
16  
17  
18  
19  
20  
21  
22  
23  
24  
25  
26  
27  
28  
29  
30  
31  
32  
33  
34  
35  
36  
37  
38  
39  
40  
41  
42  
43  
44  
45  
46  
47  
48  
49  
50  
51  
52  
53  
54  
55  
56  
57  
58  
59  
60

Membrane Lipid Composition Is Important for Plasmodesmata Function in Arabidopsis. *Plant Cell*, **2015**, 27, (4), 1228-1250.

(101) Matsunaga, S.; Yokomori, R.; Ino, D.; Yamada, T.; Kawai, M.; Kobayshi, T., EC-STM observation on electrochemical response of fluidic phospholipid monolayer on Au(111) modified with 1-octanethiol. *Electrochem. Commun.* **2007**, 9, (4), 645-650.



## Graphic Table of Content



## SYNOPSIS

The impact of electric fields on the nanoscale behavior of graphite-supported lipid monolayers was studied in solution using high resolution atomic force microscope and fluorescence recovery after photobleaching.